Journal of Power Sources 238 (2013) 413–421

Contents lists available at SciVerse ScienceDirect

Journal of Power Sources

journal homepage: www.elsevier.com/locate/jpowsour

State of charge estimation for Lithium Ion cells: Design of experiments, nonlinear identification and fuzzy observer design

Christoph Hametner*, Stefan Jakubek

Christian Doppler Laboratory for Model Based Calibration Methodologies at the Institute of Mechanics and Mechatronics, Vienna University of Technology, 1040 Vienna, Austria

HIGHLIGHTS

- A unified framework for model generation and SoC observer design is presented.
- The purely data driven approach is suitable for any type of battery chemistry.
- Model based DoE ensures proper excitation while the SoC operating range is covered.
- The fuzzy observer reduces the computational complexity of the nonlinear filter.
- The proposed concepts are validated by means of a Lithium Ion power cell.

ARTICLE INFO

Article history:
Received 8 February 2013
Accepted 7 April 2013
Available online 19 April 2013

Keywords:
State of charge estimation
System identification
Neural network models
Optimal experiment design
Kalman filter
Fuzzy observer

ABSTRACT

A new systematic approach to state of charge (SoC) observer design for battery cells is presented. It is based on a purely data driven model and a nonlinear observer constructed from it. As a key novelty, a unified and generic framework for model generation (i.e. design of experiments, nonlinear model structure) and observer parametrisation is presented. An integral part of SoC observers in hybrid electrical vehicles is a dynamic battery model which describes the nonlinear system behaviour of the cell terminal voltage. In order to enable the application of the proposed concepts for any type of battery chemistry, a data based modelling approach using the architecture of local model networks (LMNs) is proposed. As an important prerequisite, optimal model based experiment design ensures proper excitation of the system dynamics while the desired SoC operating range is covered. For SoC estimation, an augmented state space representation of the LMN is derived and the nonlinear observer design is presented. In particular, the use of a fuzzy observer is beneficial in combination with LMNs since the local observers are time-invariant which greatly reduces the complexity of the global estimator. The proposed concepts are validated experimentally by means of a Lithium Ion power cell.

1. Introduction

This work describes a new systematic approach to experiment design, nonlinear system identification and observer design for battery cells for the purpose of state of charge (SoC) estimation.

The correct determination of the state-of charge and also the related state of power is an important task in hybrid electrical vehicles (HEV). In this context, the traction battery is a complex system consisting of many single cells and an especially designed electrical circuit. Part of that circuit – and by far the most critical due to its complicated calibration – is the battery management system (BMS). This supervising control unit processes the actual status of the cells of the traction battery and shares the computed dataset with the rest of the vehicle's controllers (in particular with the hybrid control unit, HCU). It determines the major operational tasks of the traction battery as are available power and energy, high reliability (long cycle and long calendar life), and battery safety under any circumstances (i.e. use and abuse cases). Achieving these goals is widely connected to the quality of the battery management system and its interaction with the other vehicle control units [1,2].

An integral part of the BMS is a mathematical cell model which describes the nonlinear dynamic behaviour of the cell terminal voltage in dependance of the charge/discharge current. Such a model allows to predict the nonlinear system dynamics of the

* Corresponding author. Tel.: +43 1 58801 32815; fax: +43 1 58801 32899.
E-mail address: christoph.hametner@tuwien.ac.at (C. Hametner).

0378-7753/$ – see front matter
http://dx.doi.org/10.1016/j.jpowsour.2013.04.040

traction battery under the specific loads and environmental conditions and is required for SoC estimation since it is not possible to measure the SoC directly. Typical modelling approaches in the field of battery cells are:

- *Electro-chemical modelling*: Such models are based on a detailed electro-chemical description of the cell, see e.g. Refs. [3–5]. The major disadvantages of this approach are that time efficient parametrisation as well as real-time application is very complex or even not possible, c.f. Refs. [6,7].
- *Equivalent circuit models*: These models comprise a combination of RC circuits in series with an internal resistance and an ideal voltage source. However, a single equivalent circuit model cannot describe the battery operation over a large range of SoC and temperature, [7]. Consequently, an individual parametrisation for various operating conditions (temperature, SoC) is required.
- *Black/grey box techniques*: Data based modelling approaches offer a versatile structure for the identification of nonlinear systems while the real-time application is easily possible, e.g. Ref. [8].

Recent publications have addressed modelling structures for HEV calibration: In Ref. [7] a phenomenological model based on an equivalent circuit model with varying parameters is presented. The model parameters are optimised based on measured data using a genetic algorithm. Another interesting approach using state space model structures with additional hysteresis and filter states is described in Ref. [6].

A widely used approach for SoC estimation of batteries is the extended Kalman filter (EKF) in combination with an equivalent circuit model, see e.g. Refs. [9–12]. The online estimation of the SoC of a Lithium Ion cell based on an electro-chemical model can be found in Ref. [13]. A simple resistor-capacitor battery model is used in Ref. [14] where modelling errors caused by the simple model are compensated by a sliding mode observer. In Ref. [8] the battery is modelled using a radial basis function neural network and the state of charge estimation based on the EKF is presented. In order to apply the EKF to the proposed nonlinear model, the battery model must be linearised at every sampling instance. A very similar approach can be found in Ref. [15]. In Ref. [6] the modelling and identification of a state space structure which includes terms that describe the dynamic contributions due to open circuit voltage, ohmic loss, polarization time constants is described. Again, an EKF is used to estimate the SoC.

In this paper, a systematic and integrated approach to cell modelling and the associated nonlinear observer design is presented and the results are validated by means of real measurement data from a Lithium Ion cell. However, the proposed method aims at time efficient modelling procedure suitable for different cell types/chemistries and the subsequent automated observer design based on the nonlinear cell model. Therefore, a data based modelling approach is chosen due to the applicability for various types of batteries. Additionally, the proposed nonlinear model structure allows for an efficient and automated nonlinear observer design. The systematic approach to SoC observer design presented in this paper can be subdivided into three steps:

- *Optimal experiment design*: Experiment design is an important prerequisite for data based modelling and has the goal to gain maximum of information from an unknown system with minimum experimentation effort. Especially with battery cell modelling, the design of experiments (DoE) plays an important role due to the fact that the SoC excitation (and the SoC operating range) directly depends on the excitation signal of the cell current. In this work, a model based experiment design methodology for battery cells is presented, where the generation of the excitation signal is particularly adjusted to the system in that a prior process model is available, see also Ref. [16]. In general, the target of model based DoE is that parameters belonging to a specific model structure can be estimated from measured data with minimal variance [17]. In addition, the optimal experiment design procedure helps to reduce time and costs for cell testing.
- *Nonlinear system identification*: The SoC observer design is based on a nonlinear model of the battery. In the context of data based modelling, local model networks (LMNs) are a widely used concept in automotive industry, see e.g. Refs. [18–20]. These models interpolate between different local models, each valid in a certain operating regime, see e.g. Refs. [21,22]. They offer a versatile structure for the identification of nonlinear dynamic systems and the incorporation of prior (physical) knowledge is easily possible due to the transparency of the LMN architecture. In the context of cell modelling, special effects such as relaxation and hysteresis impose an additional challenge. Thus, the based on Ref. [23] (and Ref. [24] respectively), the adaptation and extension of LMN structures for cell identification is addressed in this paper.
- *Nonlinear observer design*: LMNs offer local interpretability such that local linear battery impedance models can be extracted and thus provide a basis for automated nonlinear observer design. In this work, fuzzy observer design based on the proposed model structure for the purpose of SoC estimation is presented. The fuzzy observer uses standard Kalman filter theory for each local linear state space model. Linear combinations of the local filters are then used to derive a global filter [25]. The biggest advantage compared to the widely used extended Kalman filter is that the local observers are time-invariant and no linearisation at every sampling instance is required, which greatly reduces the computational complexity of the global filter.

The remainder of this paper is structured as follows: In Section 2, SoC determination in general and the SoC observer architecture is addressed. In Section 3, the battery cell modelling workflow including model based experiment design is presented. Additionally, the architecture of the LMN and the training algorithm shortly reviewed. Design and architecture of the fuzzy observer are described in Section 4. The proposed concepts are validated by means of real measurement data from a Lithium Ion cell.

2. Nonlinear SoC observer

In this section, SoC determination in general and model based SoC estimation using different observer structures are discussed.

Basically, there are two practical approaches how to determine the SoC in a mobile battery [26]: One is the relative SoC determination where an initial SoC is adjusted by taking the time integral of the current:

$$\mathrm{SoC}(t) = \mathrm{SoC}_0 + \int_{\tau=0}^{t} \frac{\eta_\mathrm{I}(I)I(\tau)}{C_\mathrm{n}} \mathrm{d}\tau \tag{1}$$

where SoC_0 denotes the initial SoC, $I(t)$ the instantaneous cell current, C_n the nominal cell capacity and $\eta_\mathrm{I}(I)$ is the coulombic efficiency. The drawbacks of this method are that the initial SoC has to be known and that the relative SoC determination becomes unreliable when operated in this mode for an extended time. Additionally, the internal resistance of the battery causes thermal energy losses upon (dis-)charging.

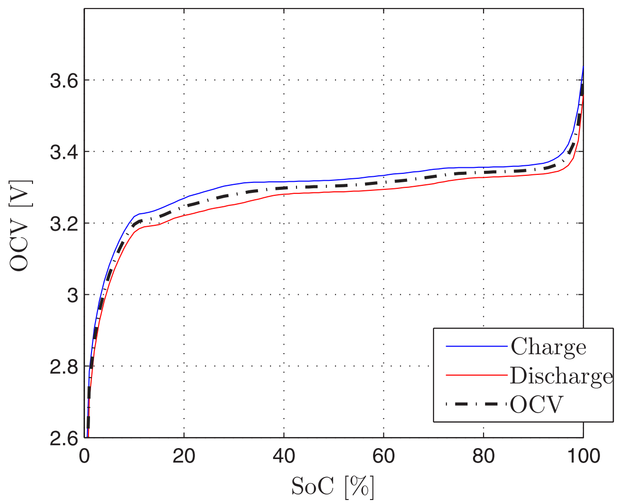

Fig. 1. OCV measurement during charging and discharging.

Secondly, it is possible to use the open circuit voltage (OCV) of a battery cell for an absolute SoC estimation. Since the open circuit voltage is the only measurable battery-intrinsic variable, this approach is more precise in most cases. However, it is not possible to directly determine the SoC using the OCV when the unit is under operation, due to a hysteresis between the charging and discharging voltage profile which depends on the load current. In Fig. 1 the OCV–SoC characteristics and the hysteresis between charging and discharging is depicted.

SoC estimation is typically based on a nonlinear model using Kalman filter theory. The nonlinear model describes the dynamic behaviour of the terminal voltage in dependance of the charge/discharge current $I(t)$ and other factors like e.g. SoC. The SoC observer is based on a combination of the (relative) SoC model (1) and the terminal voltage model, see Fig. 2. Thus, the SoC correction is obtained from a comparison of the actual terminal voltage $U(t)$ to the output of the model.

In combination with the proposed LMN different observer structures can be used, where the architecture and interpretability of the local models as a local linearisation of the process helps to reduce the model/observer complexity. These observer structures include e.g. the extended Kalman filter, the interacting multiple models (IMM) algorithm and the fuzzy observer.

The idea of the extended Kalman filter is to apply conventional Kalman filtering to a nonlinear system. The filter gain is computed using the local Jacobian of the nonlinear model. The main disadvantage of this strategy is that the filter gains cannot be precomputed since they depend on data (local linearisation), see e.g. Refs. [9,6].

The basic idea of the interacting multiple models approach is to run a certain number of different linear Kalman filters in parallel,

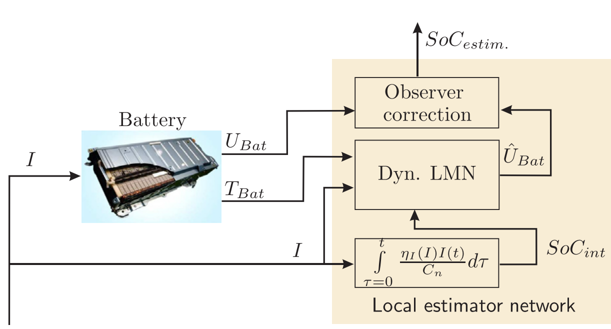

Fig. 2. Schematics of SoC observer architecture.

each corresponding to a separate model [27]. Mixing of model parameters as well as switching between the linear models is possible. The determination of the currently valid model is realized by a detection scheme, utilizing the validity probability of the underlying models [28].

In combination with LMNs, the architecture of the fuzzy observer (see e.g. Refs. [25,29–31]) helps to reduce the computational complexity of the global nonlinear filter. Each of the local models in an LMN is a linear time-invariant dynamic system. Therefore, a local observer is designed for each local linear state space model using standard Kalman filter theory. The global filter is then derived from a linear combination of the local filters.

3. Battery cell model identification

In this section the nonlinear system identification of battery cells for the purpose of SoC estimation is presented. The nonlinear model describes the dynamic behaviour of the terminal voltage $U(t)$ in dependance of the charge/discharge current $I(t)$ and other factors like e.g. temperature and SoC. In the following, the requirements for the cell model for the application in HEV development are formulated (c.f. Ref. [6]):

- based only on readily available signals only (cell terminal voltage, cell current, cell external temperature),
- valid up to very high C-rates (±20C),
- highly accurate even under strong dynamic excitation,
- includes special effects such as hysteresis and relaxation,
- suitable for real-time applications.

As an important prerequisite for nonlinear system identification, a model based experiment design procedure for battery cells is presented in Section 3.1. In Section 3.2, the LMN architecture is briefly described and adapted for battery cell modelling in order to take into account hysteresis and relaxation. The proposed concepts are then validated using real measurement data from a high power Lithium Ion cell.

3.1. Optimal experiment design

An important prerequisite for data based modelling approaches is a suitable experiment design. In general, the target of the DoE is to generate informative data while the experimentation effort is reduced. Thus, the experiment design can be understood as a compromise between experimentation effort, reliability and accuracy under the specific loads and environmental conditions.

In the context of cell modelling, the whole operating range (cell current, SoC) of the cell has to be covered and the model has to be accurate for a highly dynamic excitation (high C-rates). One of the main challenges regarding the experiment design, is that the SoC excitation (and the operating range) directly depends on the excitation signal of the cell current, c.f. Equation (1). In nonlinear system identification, amplitude modulated pseudorandom binary signals (APRBS) [19] are widely used in order to track the nonlinearities of the underlying process. This strategy is no longer feasible for the excitation of battery cells since the dependence between cell current and SoC is not taken into account which leads to insufficient coverage of the operating range of the battery. Consequently, the experiment design has to assure that the variation of the cell current on the one hand yields a proper excitation of the cell and on the other hand that the desired SoC operating range is covered. Additionally, the time for battery testing has to be taken into account in the optimisation procedure. In this work, a model based experiment design approach is presented which is especially suited for cell model identification.

3.1.1. Model based DoE

In general, model based design of experiments is a methodology for the generation of excitation signals, where the signal is adjusted to a specific prior process model in a way that the model parameters can be estimated from measured data with minimal variance, see e.g. Refs. [17,32]. The optimisation can be based on linear (e.g. obtained from preliminary tests) or nonlinear dynamic models (from a similar battery cell). In the present work, a linear dynamic cell model, which was identified from preliminary tests (step responses), was used for optimal experiment design. However, the results presented later in this section indicate that even such a simple prior process model helps to improve the model quality significantly.

In order to maximise the information of the excitation signal, the Fisher information matrix (FIM) is used [33]. In statistical terms the Fisher information matrix $\mathcal{I}$ is a tool to measure the information content of the excitation signal. The FIM is a real valued and symmetric matrix, whose inverse yields a lower bound for the parameter covariance matrix. The definition of the FIM is based on the partial derivative of the model output with respect to the model parameters, c.f. Ref. [32]:

$$\mathcal{I} = \frac{1}{\sigma^2}\sum_{k=1}^{N}\frac{\partial\hat{y}(k,\boldsymbol{\theta})}{\partial\boldsymbol{\theta}}\frac{\partial\hat{y}(k,\boldsymbol{\theta})}{\partial\boldsymbol{\theta}}^T \tag{2}$$

For the optimisation of the input signal, a scalar criterion J is required. In this context, the D-optimality criterion is widely used where the determinant of the FIM is subject to maximization:

$$J_{\mathrm{FIM}} = \det(\mathcal{I}). \tag{3}$$

The optimisation of the cell current excitation signal is based on the following predefined conditions:

- *SoC operating range*: To assure a proper coverage of the SoC operating range (and to observe SoC limits), predefined SoC levels have to be included in the experiment design.
- *Cell current excitation*: To obtain a proper distribution of the cell current excitation predefined current levels are applied. Thus, even when the optimisation is based on a linear cell model, a good coverage of the input space is obtained.
- *Hysteresis and relaxation*: In order to capture the voltage hysteresis and relaxation behaviour of the battery cell, the charge/discharge pulses are followed by zero current phases.

Thus, the excitation signal is obtained from a certain number of design points, each characterised by the absolute value of their cell current and SoC level. The target of the optimisation procedure is to determine an optimal sequential arrangement of these points. For each design point, the sign of the cell current (charging or discharging) and the duration of the charge/discharge pulse is obtained from the associated/desired SoC level and the previous SoC. Hence, the testing time directly depends on the sequential arrangement of the SoC levels and the associated current levels. As a consequence, the duration of the testbed run is also subject to optimisation (in addition to the information content of the signal).

The optimisation is focused on the appropriate sequential arrangement of the SoC levels and a proper assignment of the current levels using the simulated annealing method. Similar to Ref. [34] the search begins with an initial design and proceeds through examination of a sequence of designs, each generated as a perturbation of the preceding one. Thus, a new candidate state is obtained from a random exchange of the current and SoC levels, respectively. The probability of making a transition from the current state to the new state is specified by an acceptance probability function.

In order to optimise the information content of the signal while the testing time is kept to a minimum, the following performance function is minimised

$$J_{\mathrm{opt}} = \alpha\frac{J_{\mathrm{FIM,init}}}{J_{\mathrm{FIM,opt}}} + (1-\alpha)\frac{T_{\mathrm{opt}}}{T_{\mathrm{init}}} \tag{4}$$

where $J_{\mathrm{FIM,init}}$ denotes the determinant of the Fisher information matrix of the initial design and T_{init} and T_{opt} are the duration of testbed run of the initial and the optimised design. The choice of the design parameter $0 \le \alpha \le 1$in Equation (4) is based on the tradeoff between accuracy and measurement effort: When α is increased the information content is increased, while for $\alpha = 0$ only the testing time is reduced. Note that, on the one hand, an increasing number of data also leads to an improvement of Equation (3). On the other hand, the number of data cannot be arbitrarily decreased since the predefined SoC and current levels have to be included in the design.

3.1.2. Experimental results

The proposed concepts presented in this paper are validated by means of a Lithium Ion cell. Therefore, two training data records (obtained from the initial experiment design and the optimised input signal) and a validation dataset were recorded. In this section, measured input and output data and the results from the optimisation in Section 3.1.1 obtained from an initial design and the associated optimised design are presented.

The complete initial data record is shown in Fig. 3, where the initial value of "Charge [Ah]" corresponds to 80% SoC. The nominal capacity of the power cell is 2 Ah and the nominal voltage 3.3 V, respectively. Accordingly, the SoC operating range is between 20% and 80%. Note that the choice of the initial sequential arrangement of the SoC levels plays an important role for the testing time T_{init} of the initial dataset.

The initial design was then used as a starting point for the optimisation of Equation (4) using the simulated annealing algorithm. Here, the initial and final SoC were fixed and thus not subject to optimisation. In Fig. 4 the improvement of the determinant of the Fisher information matrix and the reduction of the measurement time are depicted. Obviously, the determinant Equation (3) is

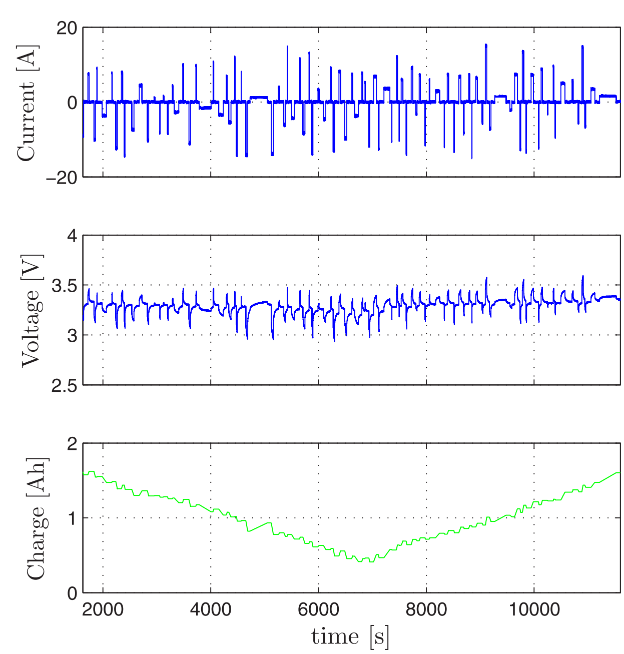

Fig. 3. Training data record: initial DoE.

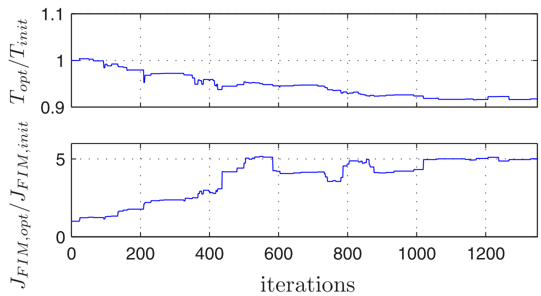

Fig. 4. Optimisation of the excitation signal using simulated annealing.

increased by a factor of five while the testing time is reduced by about 7%.

The measured data record obtained using the optimised input signal is presented in Fig. 5. Again the SoC operating range is between 20% and 80% and the predefined current levels are realised.

3.2. Nonlinear system identification

In this section, the identification of the Lithium Ion power cell from the data presented in Section 3.1 is presented. The input into the model are the cell current I and its past values up to an order of four, the state of charge SoC $(k-1)$ and the model output is the cell terminal voltage $U(k)$. For the feasibility study presented in this paper, the cell temperature is kept constant.

The architecture and training algorithm of the proposed LMN is shortly reviewed, see also Ref. [23]. Additionally, the adaptation and extension of LMN structures for cell identification (in order to take into account hysteresis and relaxation) is addressed. Simulation results using measurement data from the Lithium Ion cell demonstrate the performance of the proposed model architecture.

3.2.1. Local model network architecture

The LMN interpolates between different local models, each valid in a certain region of the input space. Thus the battery cell model is based on a partitioning into several local operating regimes, represented by the dominant influence e.g. SoC, temperature, etc. This strategy allows to capture the highly nonlinear dynamic complexity in a computationally efficient way.

Each local model of the LMN – indicated by subscript i – consists of two parts: The validity function $\Phi_i(\tilde{x}(k))$ and its model parameter vector $\boldsymbol{\theta}_i$. Thereby, Φ_i defines the region of validity of the i-th local model.

The local estimate for the output is obtained by

$$\hat{y}_i(k) = \boldsymbol{x}^T(k)\boldsymbol{\theta}_i, \tag{5}$$

where $\boldsymbol{x}^T(k)$ denotes the regressor vector. In dynamic system identification, the regressor vector $\boldsymbol{x}(k)$ comprises past system inputs and outputs.

All local estimations $\hat{y}_i(k)$ are used to form the global model output $\hat{y}(k)$ by weighted aggregation

$$\hat{y}(k) = \sum_{i=1}^{M} \Phi_i(k)\hat{y}_i(k), \tag{6}$$

where

$$\Phi_i(k) = \Phi_i(\tilde{\boldsymbol{x}}(k)) \tag{7}$$

and M denotes the number of local linear models. Thereby, the elements in $\tilde{\boldsymbol{x}}(k)$ span the so-called partition space and are chosen on the basis of prior knowledge about the process and the expected structure of its nonlinearities. Thus, the dimension of the partition space and furthermore the complexity of the optimisation problem can thus be reduced dramatically, see also Ref. [19].

The computation of the validity functions Φ_i is based on a logistic discriminant tree. In Fig. 6 a model tree with three local models is depicted. Each node corresponds to a split of the partition space into two parts and the free ends of the branches represent the actual local models with their parameter vector $\boldsymbol{\theta}_i$ and their validity functions Φ_i. The overall nonlinear model thus comprises M local models and $M-1$ nodes which determine their regions of validity.

For the representation of the discriminant function in the d-th node a logistic sigmoid activation function is chosen, c.f. Ref. [35]:

$$\varphi_d(\tilde{\boldsymbol{x}}(k)) = \frac{1}{1+\exp(-a_d(\tilde{\boldsymbol{x}}(k)))} \tag{8}$$

with

$$a_d(\tilde{\boldsymbol{x}}(k)) = \begin{bmatrix} 1 & \tilde{\boldsymbol{x}}^T(k) \end{bmatrix} \begin{bmatrix} \psi_{d0} \\ \tilde{\boldsymbol{\psi}}_d \end{bmatrix}. \tag{9}$$

Here, $\tilde{\boldsymbol{\psi}}_d^T = [\psi_{d1} \dots \psi_{dp}]$ denotes the weight vector and ψ_{d0} is called bias term. The discriminant functions φ_d are used to calculate the validity functions Φ_i, c.f. Ref. [36].

The validity functions for the layout in Fig. 6 are obtained by

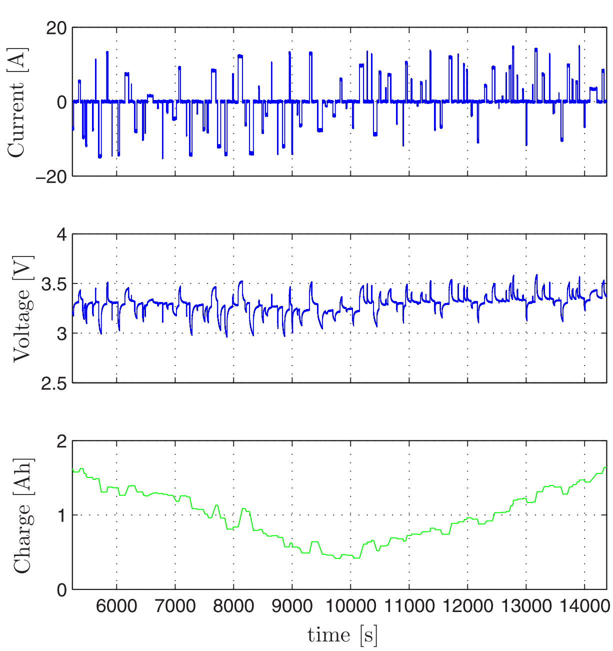

Fig. 5. Training data record: optimal model based DoE.

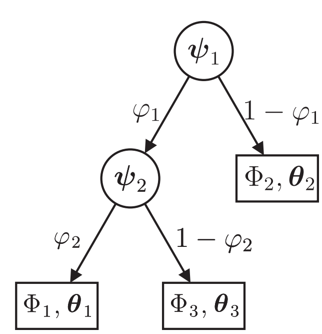

Fig. 6. Logistic discriminant tree.

$$\Phi_1 = \varphi_1\varphi_2, \tag{10}$$

$$\Phi_2 = 1-\varphi_1, \tag{11}$$

$$\Phi_3 = \varphi_1(1-\varphi_2). \tag{12}$$

An incremental model construction allows to gradually increase the complexity of the local model network: When the number of local models M is increased by one, the worst local model (indexed by l) of the logistic discriminant tree in Fig. 6 is replaced by a new node and two adjoining local models are appended, see Fig. 7. On the one hand this strategy allows a proper initialisation of the new model parameters while on the other hand the computational demand is low.

In order to reduce the computational demand, only the weight vector of the new node ψ_{M-1} is optimised while all other weight vectors are retained.

An important topic in nonlinear system identification with local model networks is the interpretability of the local models, see e.g. Refs. [37–39]. Only consequent parameters obtained by local estimation (weighted least squares) allow the interpretation of the consequent parameters as a local linearisation of the nonlinear system [39]. In order to obtain an interpretable model structure for the proposed LMN, the following cost function is chosen for the optimisation of the two new local models and the weight vector of the new node:

$$\begin{aligned} J &= \frac{1}{2}\sum_{k=1}^{N} \Phi_l(k)[y(k)-\hat{y}_l(k)]^2 + \Phi_M(k)[y(k)-\hat{y}_M(k)]^2 \\ &= \frac{1}{2}\sum_{k=1}^{N} e_l^2(k)+e_M^2(k), \end{aligned} \tag{13}$$

where

$$e_l(k) = \sqrt{\Phi_l(k)}[y(k)-\hat{y}_l(k)] \tag{14}$$

and

$$e_M(k) = \sqrt{\Phi_M(k)}[y(k)-\hat{y}_M(k)] \tag{15}$$

are the weighted local prediction errors of the adjoining models l and M, respectively. In Equation (13) N defines the number of training data.

Note that the particular choice of Equation (13) aims at a locally weighted least squares optimisation of the consequent parameters so that local interpretability is conserved.

3.2.2. Extended model structure

LMNs offer a versatile structure for the identification of nonlinear dynamic systems. Due to the transparency of the LMN architecture, the incorporation of prior knowledge is easily possible.

In order to take into account special effects such as hysteresis and relaxation, the structure of the LMN is adapted/extended:

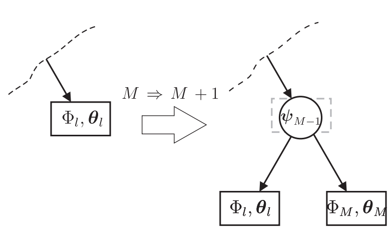

Fig. 7. Incremental tree construction.

1. The values for the resistance and capacitance of a cell model are functions of the direction of current and SoC, [7]. Thus, separate models for charge and discharge are enforced to approximate the voltage hysteresis. The architecture of LMNs allows an easy integration of this dependency using a user-defined pre-partitioning based on the current direction sign(i).
2. In Refs. [6], large time constants which describe the relaxation effect are implemented as a low-pass filter on $I(k)$. Accordingly, an additional input

$$v = \text{filt}(I) \tag{16}$$

for the LMN is used in this work. The filt-operator in Equation (16) represents a low-pass filter with zero dc gain. Here, zero dc gain ensures that the influence of the additional input vanishes after a rest period so that the model output converges to OCV, c.f. Ref. [6].

3.3. Modelling results

The performance of the LMN is highlighted using real measurement data from the Lithium Ion power cell. The training of the LMN using the algorithm presented in Section 3.2.1 results in an LMN with 20 local linear models. In order to prove the generalisation capabilities of the proposed LMN validation data were recorded, see Fig. 8. Here, the current profile was taken from Ref. [7] and adjusted in a way that the desired SoC operating range is covered. Again, the initial value of “Charge [Ah]” corresponds to 80% SoC.

In Fig. 9 a comparison of measured and simulated model output at validation is depicted. It is clearly visible that the LMN accurately describes the nonlinear behaviour of the cell while the SoC is varied in a wide range.

In Table 1 the performance of the models obtained from initial and the optimised DoE is indicated by means of the R^2 statistics

$$R^2 = 1-\frac{\sum_{k=1}^{N}(y(k)-\hat{y}(k))^2}{\sum_{k=1}^{N}(y(k)-\bar{y})^2}, \tag{17}$$

where $\bar{y}$ is the mean value of all $y(k)$.

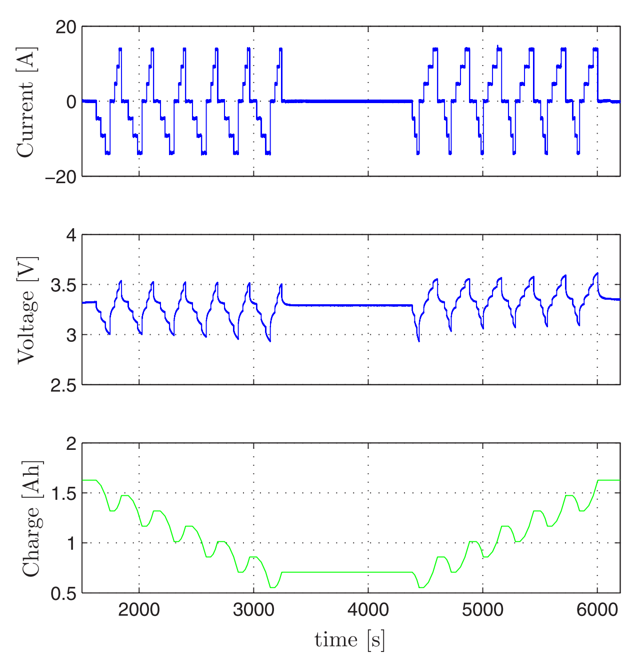

Fig. 8. Validation data record.

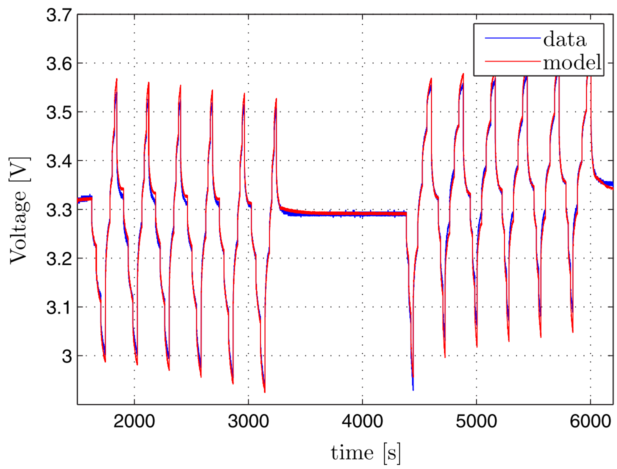

Fig. 9. Comparison of simulated model output and measured terminal voltage (validation).

4. Fuzzy observer based SoC estimation

The architecture and interpretability of LMNs (see Section 3.2.1) provides a framework for automated nonlinear observer design. Especially, the use of a fuzzy observer is beneficial in combination with LMNs: Each of the local models in an LMN is a linear time-invariant dynamic system. Therefore, a local observer is designed for each local linear state space model using standard Kalman filter theory. The global filter is then derived from a linear combination of the local filters [25]. Thus, the local observers are time-invariant which greatly reduces the computational complexity of the global filter compared to the widely used extended Kalman filter. Another important advantage of the fuzzy observer architecture is that the stability analysis of the nonlinear observer is possible based on Lyapunov stability theory, see e.g. Refs. [40,41].

In this section, the fuzzy observer is shortly reviewed and simulation results from the Lithium Ion cell are presented.

4.1. Fuzzy observer design

For nonlinear dynamic systems described by local model networks, a fuzzy observer can be designed to estimate the state vector. The nonlinear observer design involves representation of the nonlinear system as local linear state space model [30]. Using standard Kalman filter theory, steady-state filters can be designed for each local model of the LMN and the global filter is obtained from a linear combination of the local filters.

The SoC observer is based on a combination of the (relative) SoC model Equation (1) and the terminal voltage model (see Section 3.3). Thus, an augmented state space formulation of the nonlinear model is required. Using the relation $\mathrm{SOC}(k) = \mathrm{SOC}(k-1) + T_s/C_n i(k)$ the augmented state vector Equation (18) also comprises $\mathrm{SoC}(k-1)$ which was originally used as a model input for the training of the LMN. The state vector is defined as

Table 1
Model performance at validation data.

	Initial DoE	Optimised DoE
R^2	0.98452	0.99271

$$z(k-1) = \begin{bmatrix} y(k-1) \\ y(k-2) \\ \vdots \\ y(k-n) \\ SOC(k-1) \end{bmatrix}. \tag{18}$$

With the system matrix

$$A_i = \begin{bmatrix} a_{1,i} & a_{2,i} & \dots & a_{n,i} & b_{\mathrm{SOC},i} \\ 1 & 0 & \dots & 0 & 0 \\ 0 & 1 & \dots & 0 & 0 \\ \vdots & \vdots & \ddots & \vdots & \vdots \\ 0 & 0 & \dots & 0 & 1 \end{bmatrix} \tag{19}$$

the input matrix

$$\boldsymbol{B}_i = \begin{bmatrix} b_{10,i} & b_{11,i} & \dots & b_{20,i} & b_{21,i} & \dots & b_{2m,i} & c_i \\ 0 & 0 & \dots & 0 & 0 & \dots & 0 & 0 \\ \vdots & \vdots & \ddots & \vdots & \vdots & \ddots & \vdots & \vdots \\ \frac{T_s}{C_n} & 0 & \dots & 0 & 0 & \dots & 0 & 0 \end{bmatrix} \tag{20}$$

and the input vector which contains current and past elements of the inputs

$$\boldsymbol{u}(k) = \begin{bmatrix} i(k) \\ i(k-1) \\ \vdots \\ v(k) \\ v(k-1) \\ \vdots \\ v(k-m) \\ 1 \end{bmatrix}. \tag{21}$$

the state equation of the ith local model is obtained

$$\boldsymbol{z}(k) = \sum_{i=1}^{M} \Phi_i(k-1)\{\boldsymbol{A}_i \boldsymbol{z}(k-1) + \boldsymbol{B}_i \boldsymbol{u}(k)\}. \tag{22}$$

The system matrix Equation (19) and the input matrix Equation (20) comprise the elements of the numerator and denominator polynomials and the affine term c_i of the local affine models.

With $C = [10\dots00]$ the global model output is obtained

$$y(k) = \boldsymbol{C}\boldsymbol{z}(k) \tag{23}$$

Using these relations, a local steady-state Kalman filter with the gain matrix $\boldsymbol{K}_i$ can be designed for each local model. The overall state estimation is then defined as a weighted sum of the individual linear observers. The state estimate $\hat{\boldsymbol{z}}(k)$ is given by the following equations:

$$\boldsymbol{z}_i^*(k) = \boldsymbol{A}_i \hat{\boldsymbol{z}}(k-1) + \boldsymbol{B}_i \boldsymbol{u}(k) \tag{24}$$

and

$$\hat{\boldsymbol{z}}(k) = \sum_{i=1}^{M} \Phi_i(k-1)\{\boldsymbol{z}_i^*(k) + \boldsymbol{K}_i[y(k) - \hat{y}(k)]\} \tag{25}$$

where

$$\hat{y}(k) = \sum_{i=1}^{M} \Phi_i(k-1)\boldsymbol{C}\boldsymbol{z}_i^*(k) \tag{26}$$

The Kalman gain matrix $\boldsymbol{K}_i$ is obtained from

$$\boldsymbol{K}_i = \boldsymbol{A}_i\boldsymbol{P}_i^T\boldsymbol{C}^T\left(\boldsymbol{C}\boldsymbol{P}_i^T\boldsymbol{C}^T + \boldsymbol{R}^T\right)^{-1} \tag{27}$$

where $\boldsymbol{P}_i$ is the solution of the discrete-time algebraic Riccati equation (DARE)

$$\boldsymbol{A}_i\boldsymbol{P}_i\boldsymbol{A}_i^T - \boldsymbol{P}_i - \boldsymbol{A}_i\boldsymbol{P}_i\boldsymbol{C}^T\left(\boldsymbol{C}\boldsymbol{P}_i\boldsymbol{C}^T + \boldsymbol{R}\right)^{-1}\boldsymbol{C}\boldsymbol{P}_i\boldsymbol{A}_i^T + \boldsymbol{Q} = 0 \tag{28}$$

Here, $\boldsymbol{Q}$ and $\boldsymbol{R}$ denote the covariance matrices of the measurement noise $\boldsymbol{\nu}$ and of the process noise $\boldsymbol{\mu}$, respectively. In Kalman filter theory, the covariance of both the process and measurement noise are assumed to be known. However, the covariance matrices are often used as a design parameter since in practice the covariance values are not precisely known. In the present application, the covariance matrix of the measurement noise $\boldsymbol{R}$, can be estimated from the knowledge of the battery terminal voltage. Similar to Ref. [9], $\boldsymbol{Q}$ is obtained from experimental studies under the simplifying assumption that there is no correlation between the elements of $\boldsymbol{\mu}$. In the next section, SoC estimation results presented where the covariance value of SoC is used as a tuning parameter for the nonlinear SoC observer.

4.2. SoC estimation results

The performance of the fuzzy observer for SoC estimation is demonstrated by means of the validation data record (c.f. Section 3.3). Now, the SoC is assumed to be unknown and the initial state of SoC is chosen at random.

The upper plot in Fig. 10 shows a comparison of true and estimated SoC of the Lithium Ion cell. The estimated SoC converges to the correct value even though the initialisation is chosen outside of the operating area of the training data. Obviously, the LMN based fuzzy observer accurately estimates the unknown SoC and an estimation error smaller than ±3% is obtained.

In Fig. 11 the weighting of SoC is increased in order to obtain a faster convergence after a poor initialisation. Thus, on the one hand a fast SoC error correction is obtained while on the other hand, the width of the SoC estimation error band due to modelling errors and measurement noise is slightly increased.

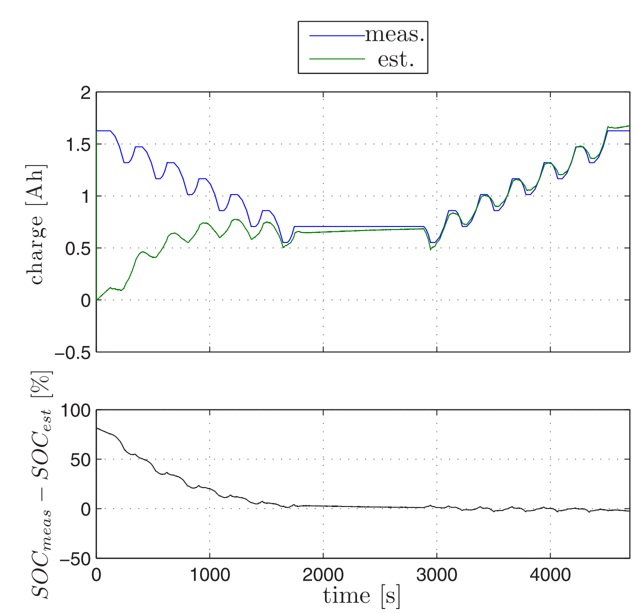

Fig. 10. Generalisation data: SoC estimation/correction after random initialisation

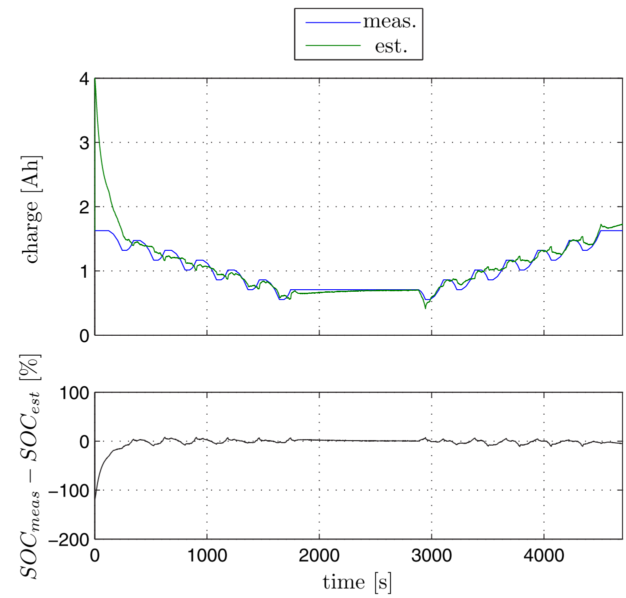

Fig. 11. Generalisation data: SoC estimation/correction after random initialization.

5. Conclusion

The work described in the present paper shows an integrated methodology for experiment design, nonlinear system identification and nonlinear observer design of a Lithium Ion power cell for the purpose of SoC estimation. Model based design of experiments for battery cells is proposed. The results indicate that even a simple prior process model helps to improve the model quality significantly while the testing time is reduced and the coverage of the SoC operating range is ensured. The local model network construction and architecture is shortly reviewed and adapted for battery modelling in order to take into account hysteresis and relaxation effects. Results obtained from real measurement data show the excellent generalisation capabilities of this approach. Additionally, the architecture and interpretability of the LMN provides a framework for fuzzy observer design. A local observer is designed for each local linear state space model using standard Kalman filter theory and the global filter is then derived from a linear combination of the local filters. Thus, the computational complexity of the global filter is greatly reduced compared to the widely used extended Kalman filter. Again, the performance of the proposed fuzzy observer is demonstrated by means of real measurement data.

Acknowledgements

This work was supported by the Christian Doppler Research Association and AVL List GmbH, Graz.

References

[1] D. Lim, A. Anbuky, A Can-based Battery Management Network: Design, Analysis, Modelling and Simulation, in: Proceedings 2004 IEEE International Workshop on Factory Communication Systems, 2004, pp. 291–295, http://dx.doi.org/10.1109/WFCS.2004.1377727.

[2] J. Chatzakis, K. Kalaitzakis, N. Voulgaris, S. Manias, IEEE Transactions on Industrial Electronics 50 (5) (2003) 990–999, http://dx.doi.org/10.1109/TIE.2003.817706.

[3] P. Arora, M. Doyle, A.S. Gozdz, R.E. White, J. Newman, Journal of Power Sources 88 (2) (2000) 219–231, http://dx.doi.org/10.1016/S0378-7753(99)00527-3.

[4] R. Klein, N. Chaturvedi, J. Christensen, J. Ahmed, R. Findeisen, A. Kojic, State Estimation of a Reduced Electrochemical Model of a Lithium-ion Battery, in: American Control Conference (ACC) 2010, 2010, pp. 6618–6623.

[5] P.M. Gomadam, J.W. Weidner, R.A. Dougal, R.E. White, Journal of Power Sources 110 (2) (2002) 267–284, http://dx.doi.org/10.1016/S0378-7753(02)00190-8.

[6] G.L. Plett, Journal of Power Sources 134 (2) (2004) 262–276, http://dx.doi.org/10.1016/j.jpowsour.2004.02.032.
[7] Y. Hu, B.J. Yurkovich, S. Yurkovich, Y. Guezennec, ASME Conference Proceedings 2009 (48937) (2009) 233–240, http://dx.doi.org/10.1115/DSCC2009-2610.
[8] M. Charkhgard, M. Farrokhi, IEEE Transactions on Industrial Electronics 57 (12) (2010) 4178–4187, http://dx.doi.org/10.1109/TIE.2010.2043035.
[9] A. Vasebi, M. Partovibakhsh, S.M.T. Bathaee, Journal of Power Sources 174 (1) (2007) 30–40, http://dx.doi.org/10.1016/j.jpowsour.2007.04.011. Hybrid Electric Vehicles.
[10] A. Vasebi, S. Bathaee, M. Partovibakhsh, Energy Conversion and Management 49 (1) (2008) 75–82, http://dx.doi.org/10.1016/j.enconman.2007.05.017.
[11] J. Han, D. Kim, M. Sunwoo, Journal of Power Sources 188 (2) (2009) 606–612, http://dx.doi.org/10.1016/j.jpowsour.2008.11.143.
[12] B. Bhangu, P. Bentley, D. Stone, C. Bingham, IEEE Transactions on Vehicular Technology 54 (3) (2005) 783–794, http://dx.doi.org/10.1109/TVT.2004.842461.
[13] S. Santhanagopalan, R.E. White, Journal of Power Sources 161 (2) (2006) 1346–1355, http://dx.doi.org/10.1016/j.jpowsour.2006.04.146.
[14] I.-S. Kim, Journal of Power Sources 163 (1) (2006) 584–590, http://dx.doi.org/10.1016/j.jpowsour.2006.09.006. Special issue including selected papers presented at the Second International Conference on Polymer Batteries and Fuel Cells together with regular papers.
[15] Z. Chen, S. Qiu, M. Masrur, Y. Murphey, Battery State of Charge Estimation Based on a Combined Model of Extended Kalman Filter and Neural Networks, in: The 2011 International Joint Conference on Neural Networks (IJCNN), 2011, pp. 2156–2163, http://dx.doi.org/10.1109/IJCNN.2011.6033495.
[16] C. Hametner, M. Stadlbauer, M. Deregnaucourt, S. Jakubek, T. Winsel, Engineering Applications of Artificial Intelligence 26 (1) (2013) 251–261, http://dx.doi.org/10.1016/j.engappai.2012.05.016.
[17] L. Pronzato, Automatica 44 (2) (2008) 303–325.
[18] M. Hafner, M. Schüler, O. Nelles, R. Isermann, Control Engineering Practice 8 (11) (2000) 1211–1221, http://dx.doi.org/10.1016/S0967-0661(00) 00057-5.
[19] O. Nelles, Nonlinear System Identification, first ed., Springer Verlag, 2002.
[20] C. Hametner, S. Jakubek, Combustion Engine Modelling Using an Evolving Local Model Network, in: Proceedings of the 2011 International Conference on Fuzzy Systems (FUZZ IEEE 2011) (2011).
[21] R. Murray-Smith, T.A. Johansen, Multiple Model Approaches to Modelling and Control, Taylor & Francis, 1997.
[22] G. Gregorcic, G. Lightbody, IEEE Transactions on Neural Networks 18 (5) (2007) 1404–1423, http://dx.doi.org/10.1109/TNN.2007.895825.
[23] C. Hametner, S. Jakubek, Neuro-fuzzy Modelling Using a Logistic Discriminant Tree, in: American Control Conference, 2007. ACC '07, 2007, pp. 864–869, http://dx.doi.org/10.1109/ACC.2007.4283048.
[24] S. Jakubek, C. Hametner, IEEE Transactions on Systems, Man, and Cybernetics, Part B: Cybernetics 39 (5) (2009) 1121–1133, http://dx.doi.org/10.1109/TSMCB.2009.2013132.
[25] D. Simon, Applied Soft Computing 3 (3) (2003) 191–207, http://dx.doi.org/10.1016/S1568-4946(03)00034-6.
[26] V. Pop, H.J. Bergveld, P.H.L. Notten, P.P.L. Regtien, Measurement Science and Technology 16 (12) (2005) R93–R110.
[27] E. Mazor, A. Averbuch, Y. Bar-Shalom, J. Dayan, IEEE Transactions on Aerospace and Electronic Systems 34 (1) (1998) 103–123, http://dx.doi.org/10.1109/7.640267.
[28] S. Helm, M. Kozek, S. Jakubek, IEEE Transactions on Industrial Electronics 59 (11) (2012) 4326–4337, http://dx.doi.org/10.1109/TIE.2012.2193855.
[29] G. Chen, Q. Xie, L.S. Shieh, Information Sciences 109 (1–4) (1998) 197–209, http://dx.doi.org/10.1016/S0020-0255(98)10002-6.
[30] R. Senthil, K. Janarthanan, J. Prakash, Industrial & Engineering Chemistry Research 45 (25) (2006) 8678–8688, http://dx.doi.org/10.1021/ie0601753.
[31] M. Polanský, C. Ardil, International Journal of Mathematical and Computer Sciences 3 (1) (2007).
[32] G. Goodwin, R. Payne, Dynamic System Identification: Experiment Design and Data Analysis, in: Mathematics in Science and Engineering, vol. 136, Academic Press, 1977.
[33] S.M. Kay, Fundamentals of Statistical Signal Processing: Estimation Theory, Prentice Hall Inc., New Jersey, USA, 1993.
[34] M. Morris, Journal of Statistical Planning and Inference 43 (3) (1995) 381–402, http://dx.doi.org/10.1016/0378-3758(94)00035-T.
[35] C.M. Bishop, Neural Networks for Pattern Recognition, Oxford University Press, USA, 1995.
[36] P. Pucar, M. Millnert, Smooth Hinging Hyperplanes – an Alternative to Neural Networks, in: Proceedings of the 3rd ECC (1995).
[37] R. Babuska, Fuzzy Modeling for Control, Kluwer Academic Publishers, Norwell, MA, USA, 1998.
[38] T.A. Johansen, R. Shorten, R. Murray-Smith, IEEE Transactions on Fuzzy Systems 8 (3) (2000) 297–313.
[39] J. Abonyi, R. Babuska, Local and Global Identification and Interpretation of Parameters in Takagi-sugeno Fuzzy Models, in: The Ninth IEEE International Conference on Fuzzy Systems, 2000, FUZZ IEEE 2000, vol. 2, 2000, pp. 835–840, http://dx.doi.org/10.1109/FUZZY.2000.839140.
[40] K. Tanaka, T. Ikeda, H. Wang, IEEE Transactions on Fuzzy Systems 6 (2) (1998) 250–265, http://dx.doi.org/10.1109/91.669023.
[41] C. Mayr, C. Hametner, M. Kozek, S. Jakubek, Piecewise quadratic stability analysis for local model networks, in: 2011 IEEE International Conference on Control Applications (CCA), 2011, pp. 1418–1424, http://dx.doi.org/10.1109/CCA.2011.6044503.